ELSEVIER

Wear 236 (1999) 199–209

WEAR

www.elsevier.com/locate/wear

A scuffing test for piston ring/bore combinations Part I. Stearic acid lubrication

J. Galligan [a], A.A. Torrance [a,*], G. Liraut [b]

[a] *Department of Mechanical Engineering, Trinity College, Dublin 2, Ireland*
[b] *Renault, D.I. Mat, Service 60152, 92100 Boulogne-Billancourt, France*

Received 6 December 1998; received in revised form 1 July 1999; accepted 1 July 1999

Abstract

In some circumstances, the friction of boundary lubricated surfaces can become higher as they become smoother. This effect can be predicted from an elastoplastic model of asperity contact, and the properties of boundary lubricants. In this paper, the model is used to explain the results obtained during the development of a bench test to simulate the scuffing of piston rings in the bores of internal combustion engines. It is proposed that the rapid rise in friction which occurs after running a hot, sparsely lubricated contact for sufficient time is due to a combination of polishing and a modest reduction in the coverage of the rubbing surfaces by the boundary film. It can be well predicted by the model. © 1999 Elsevier Science S.A. All rights reserved.

Keywords: Scuffing test; Piston ring/bore; Internal combustion engines

1. Introduction

In elementary mechanics courses, a smooth surface is often taken to be ''frictionless''. However, the study of real sliding contacts shows that this perception can be very wide of the mark [1–4], since under some conditions, boundary friction can become high and rise, as a sliding surface becomes smoother. This leads to the surprising situation where polishing of the contact surface is a sign of its deterioration, as for example, in the contact between the top compression ring and cylinder bore in an internal combustion engine. Where brake mean effective pressure is high, the cylinder bores can sometimes suffer high polishing wear which removes the honing marks and leaves areas of mirror finish [5–7]. The wear mechanism is thought to be mainly very fine abrasion (two and three body), though plastic flow also plays a part [7]. As the degree of polishing increases, there is an increase in oil consumption, blow by of exhaust gases, and an increase in emissions, [6–9]. Eventually, friction may rise and scuffing ensues [5,6,8]. Obviously, the time taken to reach a critical state may also be influenced by the initial surface finish of the liner and ring. If they were too smooth, it is conceivable that they might not function at all.

There is as yet no satisfactory model in the literature to explain the link between polishing and scuffing. Wilson and Callow [9] considered that the cause could be associated with a change in oil distribution as honing marks wear away, or with the accumulation of degraded oil in the deep honing scratches, but they were unable to give any quantitative description of the phenomenon. One reason for this may be that, until recently, there have been no quantitative models linking surface texture (the result of polishing) and friction (whose rise is associated with scuffing), and most of those which exist predict that polishing should give low friction [10,11].

Other problems arise from the complexity of the chemistry of engine lubricants [12], which can have a profound effect on friction, and from the difficulty in making precise measurements of the friction between ring and liner in a firing engine [13]. In order to isolate the effect of polishing, and the initial surface finish of the liner on friction, some fairly simple tests could be performed to simulate the conditions at the ring/bore contact with a simple and well-defined boundary lubricant. It would then be possible to describe what occurs by using a model [4], which allows for the possibility of rising friction when surfaces become smooth; and this is the approach adopted in this paper. The test method uses a reciprocating friction machine (The Cameron-Plint TE77 machine) which allows a ring to be rubbed against a specimen cut from a cylinder bore under

* Corresponding author. Tel.: +353-1-702-1778; fax: +353-1-679-5554; E-mail: atorrnce@tcd.ie

0043-1648/99/$ - see front matter
PII: S0043-1648(99)00278-1

temperatures and loads typical of the conditions at top dead centre in an internal combustion engine. The lubricant used was a 1% solution of stearic acid in white oil. A great many boundary lubrication studies have used this lubricant [1–3,14–16], and details of the shear strength of the boundary films which result from it are available [16], so it is much easier to interpret the friction experiments than when a motor oil is used.

2. Friction model

From the foregoing remarks it can be seen that high friction in cylinder/liner contacts may occur both when the surfaces are too rough, and when they are too smooth. The friction model used in this work seems to be the only one available which fulfils both these criteria. It has been published in an earlier paper [4], but for the sake of completeness it is given here. The starting point is the model of Black et al. [17], which assumes that an asperity contact can be represented as a hard wedge that slides over a soft ductile surface, pushing a plastic wave ahead of it. Slip line fields can then be developed to predict the stress in the softer material due to the passage of a hard asperity. An example is shown in Fig. 1. The stress and strain depend on the interfacial shear strength ratio ($f = \tau/k_s$) and the angle that the hard wedge makes with the soft surface. If a real hard surface can be represented as an array of such asperities, then its friction can be calculated successfully from its *slope* distribution, a surface texture parameter, and f, a lubrication parameter [18]. The equations below give the forces per unit width of wedge [17], which can then be used to find μ:

$$F_t = (A\sin\alpha + \cos(2\varepsilon - \alpha))\mathrm{ED}\,k_s \quad (1)$$

$$F_n = (A\cos\alpha + \sin(2\varepsilon - \alpha))\mathrm{ED}\,k_s \quad (2)$$

$$\mu = \frac{F_t}{F_n} \quad (3)$$

where $A = 1 + \pi/2 + 2\varepsilon - 2\eta - 2\alpha$, $2\varepsilon = \arccos(f)$, $f = \tau/k_s$, τ being the shear strength of ED.

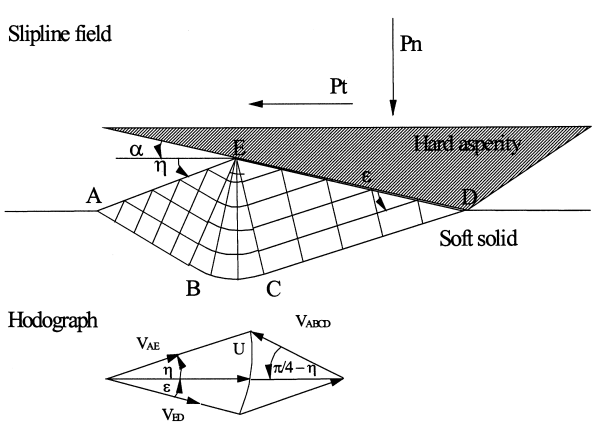

Fig. 1. Slipline field and hodograph of rigid plastic wave formation, [9].

Provided the asperity contacts are mainly plastic, the above model gives a reasonable account of the effects of changing surface texture on μ in single asperity tests [17] and for real surfaces [18]. The main conclusions are that μ should fall with surface slope, and with interfacial shear strength.

Bowden and Tabor [14,15] considered that the shear strength of the interface arose from defects of the boundary film covering the contacting surfaces, leading to local microwelds at the gaps in the film. The value of f was taken to be the fraction of the contact not covered by the boundary film. This implies that the shear strength of the boundary film itself can be ignored. However, Briscoe et al. [16] showed that boundary films do have a measurable shear strength, τ_f given by:

$$\tau_f = p\mu_0 + \tau_0 \quad (4)$$

where p is the pressure on the film. The quantity τ_0 can generally be ignored, in which case, as shown by Black et al. [17], the deformation model of Fig. 1 leads to the simple expression for μ:

$$\mu = \tan\left(\tan^{-1}\mu_0 + \alpha\right). \quad (5)$$

Eq. (5) assumes that the asperity contact is plastic. However, at low asperity slopes, elastic effects will become more important, and the contact pressure p falls. It can now be calculated by starting from the equation for the pressure under an elastic wedge indenting a half space to make an impression of width $2a$ [19]:

$$p(x) = \frac{E^*\tan\alpha}{2\pi}\ln\left[\frac{a + \sqrt{(a^2 - x^2)}}{a - \sqrt{(a^2 - x^2)}}\right] = \frac{E^*\tan\alpha}{\pi}\cosh^{-1}\left(\frac{a}{x}\right). \quad (6)$$

As $x \to 0$, $p(x) \to \infty$, so provided yielding is possible, $p(x)$ will be attenuated by plastic flow close to the tip of the wedge. An approximate value for p can be found by assuming that $p(x)$ cannot rise above the value of p deduced from Eq. (2) ($p = F_n/\mathrm{ED} = p_m$). Substituting $p(x) = p_m$ into Eq. (6) allows the lowest value of x for elastic deformation to be found as:

$$x_m = a\sqrt{1 - \left(\frac{y-1}{y+1}\right)^2} \quad \text{where } y = \exp\left(\frac{2\pi p_m}{E^*\tan\alpha}\right).$$

The mean pressure over the asperity can then be found by summing the contributions of the elastic part, between $x = a$ and $x = x_m$, and the plastic part, between $x = x_m$ and 0:

$$p = E^*\tan\alpha\left[\frac{1}{2} - \frac{x_m}{\mu a}\int_0^{x_m}\cosh^{-1}\left(\frac{a}{x}\right)\mathrm{d}x\right] + p_m\frac{x_m}{a}. \quad (7)$$

If the shear strength of the boundary film varies in the same way as p, Eq. (5) will apply, and μ will always fall

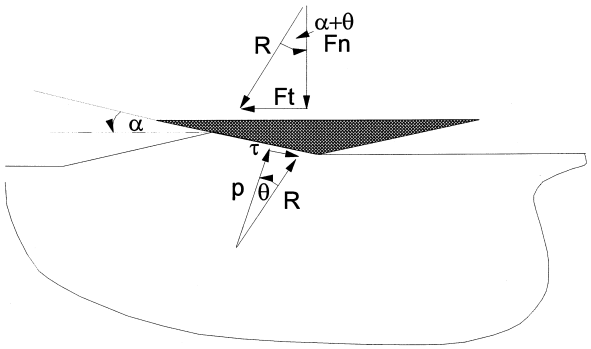

Fig. 2. Black's simplified perfectly plastic friction model, [16].

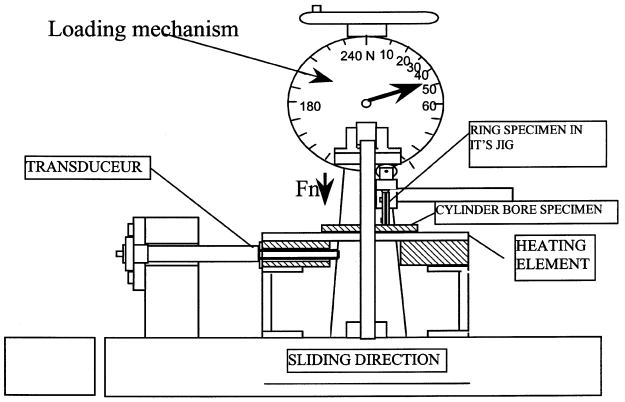

Fig. 3. Schematic of loading mechanism and ring carried in its jig and supported by the head and lever which make up the free end of the Scotch yoke assembly.

as α falls. However, if τ_0 in Eq. (4) is large enough, or if the boundary film contains defects as postulated by Bowden and Tabor [14,15] μ will rise when α falls to sufficiently low values. If both occur, Eq. (4) becomes:

$$\tau = (\mu_0 p + \tau_0)(1 - f) + k_s f. \quad (8)$$

Referring to Fig. 2 after Black et al. [17], the coefficient of friction is given by:

$$\mu = \tan(\alpha + \theta). \quad (9)$$

Where the angle θ is given by:

$$\theta = \tan^{-1}\left(\frac{\tau}{p}\right) = \tan^{-1}\left[\left(\mu_0 + \frac{\tau_0}{p}\right)(1 - f) + f\frac{k_s}{p}\right]. \quad (10)$$

Taken together, Eqs. (7)–(10) allow μ to be calculated as a function of the measured mechanical properties of boundary films, asperity slope, and the mechanical properties of the contact. The factor f represents the fractional defect of the boundary film. If it is not zero, then μ will rise when p becomes very low.

If scuffing is taken to occur when friction reaches some critical value, then these equations show that its occurrence may be related to a critical combination of surface texture (asperity slope) and boundary film breakdown (f). As the surface becomes smoother, the critical value of f needed will fall; but unless there is some film breakdown, scuffing will not occur. There is also the possibility that the time taken to reach a critical surface texture may be related to the initial finish. Thus, a test should be developed which will allow these effects to be followed and which will identify the combinations of lubrication and finish which may give rise to difficulties.

3. Experimental

The first part of this work was therefore concerned with the development of a repeatable and representative scuffing test procedure for testing cylinder bores. However, the tribological process of real engines involves complicated interactions among the piston, piston rings, cylinder bore, lubricant, and chemical environment, with conditions varying from cold start to full power output. Therefore, bench tests cannot fully simulate actual engine conditions since the contact is mechanically loaded, speeds are much lower, stroke is shorter, and the real motion of the piston ring cannot be simulated. The advantage of bench tests, however, is that they allow better monitoring and control of the different parameters, and since this work is primarily concerned with the effect of bore surface finish on friction and scuffing, it was essential that all other parameters were kept constant. The scuffing tests were carried out on a Cameron Plint TE77 tribometer, (Fig. 3), which has the advantage of allowing specimens of actual components with their original surface finish, metallurgy, and geometry to be tested.

3.1. Specimens

The tests were carried out on cast iron cylinder bore specimens and barrel profile chrome coated cast iron top compression ring specimens, the properties of which are shown in Table 1. Since piston rings are made with a free diameter larger than that of the cylinder bore to assist sealing, and because in this experimental set-up the ring is not constrained within a whole bore, the ring was chosen with a smaller diameter than that of the bore and is therefore not of the same engine. The diameter of the cylinder bore was 81 mm whilst the outer diameter of the piston ring in its free state was approximately 79 mm, (to

Table 1
Material properties of specimens

Cast iron cylinder bore	Chrome coated cast iron piston ring (data is for coating)
Hardness (average) = 200 Hv	Hardness = 990 Hv
Young's modulus = 126 GPa	Young's modulus = 289 GPa
Poisson's ratio = 0.3	Poisson's ratio = 0.3

fit an engine bore of 75.8 mm). The cylinder bore specimens were cut in rectangular sections of 45 mm by 30 mm, 3 mm thick in their centre, and were tested against sections of piston ring 75 mm in width. The specimens were cleaned with petroleum ether in an ultrasonic bath, then rinsed several times in a soxhlet extractor, and stored immediately in a desiccator.

The friction model described above predicts that these specimens tested with 1% stearic acid will have friction coefficients higher than 0.2 when the combined ring and bore RMS slope is less than 0.5°, if the lubricating film separating the surfaces is not perfect. However, it was not possible to fully test this in these tests, as the honing scores of the bore specimens need to be removed, and on materials such as cast iron the phases of graphite which lie close to the surface can become exposed after short periods of wearing, releasing graphite particles into the contact area which then intervene in the tribological process, [20]. However, other workers have verified this effect with other ferrous materials. Hirst and Hollander [2] showed experimentally that there was a critical roughness below which and above which scuffing occurred at a lower critical temperature, and Poon and Sayles [3] have confirmed their results. Nevertheless, a range of bore finishes was prepared by polishing the specimen to different degrees on a specially designed apparatus which allowed both bore specimens and piston rings to be polished with greater regularity due to a constant loading mechanism. Profile measurements were taken with a Somicronic Surfascan profilometer, and profiles were taken on both bore and ring specimens prior to testing and on the wear scars after testing. The profiles were functionally filtered with a bandwidth defined by the contact length, and the film thickness, which for boundary lubricants of this type is about 1 nm, as reasoned by Torrance and Parkinson [18]. Such a thin film is not expected to greatly influence the effective roughness of this contact, and it was subsequently found that filtering with this cut-off had little effect on the asperity angles calculated. The profiles were smoothed using a filtering technique similar to the German E-system, [21], with a contact length of 0.2 mm, which was measured with pressure sensitive film placed in the contact with the test load applied.

3.2. Test set-up

The ring is carried in a head which is located at the free end of a scotch yoke assembly, with the aid of a specially designed jig which allows the ring segment to conform to a circular shape with a diameter of 79 mm. The ring is pushed into the jig until it conforms to the circular shape, and clamped in the vertical plane. The ring is oscillated in the horizontal direction by a thyristor-controlled variable speed motor, and the frequency at which the test is carried out is regulated with a dynamo tachometer and the operating software. The cylinder bore specimen, which remains fixed throughout the test, is clamped to a heater block by means of a jig which also ensures that the centre line of the cylinder bore specimen is parallel to the movement of the ring. The ring is loaded against the cylinder bore by means of a spring balance, and the force is transmitted directly onto the oscillator head by means of a needle roller cam follower. The heater block is mounted on a flexure with heat resisting insulation blocks interposed, and the tangential force is monitored by a Kistler type 9203 piezoelectric force transducer attached to the insulating block. A Kistler type 5007 charge amplifier is connected to a force transducer and provides a d.c. voltage output proportional to the measured force. The amplifier also gives a d.c. voltage equivalent to the true RMS value of the input signal, and therefore a continuous reading of the friction force may be obtained during the test. The specimen is heated by two electric heating bars sunk into the heating block, which are controlled by a Coreci Minicor programmable electric heat regulator. Two chromel alumel thermocouples are inserted into holes drilled in the cylinder bore specimens, one of which is connected to the heat regulator while the other is linked to the data acquisition.

The test is operated by means of a software programme, which allows data acquisition to occur simultaneously. The temperature, frequency, and friction coefficient are thus recorded throughout the test as a function of time at regular intervals. The test is launched for a fixed length of time, though if scuffing occurs, which is defined by the sudden rise in friction coefficient, the test is stopped automatically as the friction coefficient is monitored throughout the test and a maximum friction coefficient is set at the start of the test as the scuffing limit. There is also a timer that stops automatically with the test, allowing accurate timing of the test.

3.3. Test parameters

The test conditions were chosen to simulate those experienced by the top compression ring just below the top dead centre on the firing stroke where scuffing has generally been found to initiate, where the lubricant film thickness is thinnest, and temperature and peak gas pressures are highest, [22]. The first difficulty was choosing a suitable load, as all available data on engine friction forces and piston thrust loads are for complete ring packs and in this set-up only the top compression ring is tested. Also, the loads exerted by the rings on the bore wall in an engine are not constant, varying with stroke and piston dynamics. However, since the objective was to induce scuffing, the maximum load at the top dead centre on the expansion stroke was chosen. This corresponds to a normal pressure of 6 MPa, and with the dimensions of the specimens tested, this corresponded to a normal load of 80 N.

Since a true simulation of engine stroke and speed is not possible with this apparatus, and since only conditions

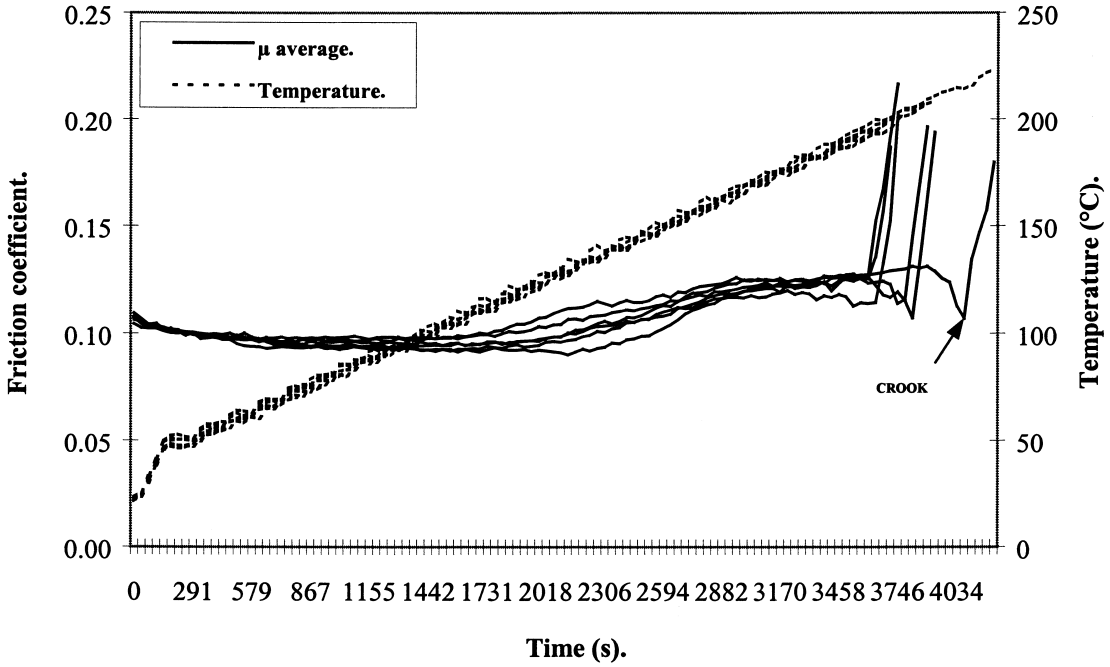

Fig. 4. Critical temperature for scuffing using 1% stearic acid in white oil.

of boundary lubrication at the top dead centre are of concern, a stroke of 5 mm and a frequency of 4.4 Hz were chosen. This short stroke also ensures that flash temperature will be negligible, and thus that the contact temperature will be accurately specified.

The most common method of lubrication in bench wear tests is to fully immerse the specimens in oil. However, this hardly simulates the sparse oil supplied by oil splash from the crankshaft, or the starved lubrication conditions due to ring interaction. Tests in immersed conditions did not result in scuffing and the quantity of lubricant applied to the contact was found to have an effect on the time to scuff, the effects of which are discussed elsewhere [20]. Therefore, the contact was smeared with 100 μl 1% stearic acid in white medicinal oil, and the specimens were allowed to stand at the test temperature for 15 min.

Boundary additives have different properties at different temperatures, and if the lubricated surfaces are slowly heated up it is found that at some critical temperature there is a marked rise in friction and wear as the boundary film breaks down. A common method therefore in boundary lubrication scuffing tests is to raise the temperature until scuffing occurs, [1,2,23]. However, it was decided to carry out the tests at constant temperature because of the changes in surface finish which are bound to occur due to the specimens running-in as the temperature is raised. Therefore, the chosen temperature had to be lower than the critical temperature of the lubricant but high enough to cause scuffing, as it is clear that scuffing is in part due to lubricant breakdown at high temperatures.

Preliminary tests were therefore carried out to find the scuffing temperature of 1% stearic acid in white oil, at 80 N and 4.4 Hz, with a 5-mm stroke, and with 100 μl 1% stearic acid in white oil and a temperature gradient of 2.5°C/min, on standard bore specimens. The results are shown in Fig. 4, and the scuffing time and temperature are taken at the crook of the friction coefficient curve, i.e., where the friction coefficient starts to increase sharply. The tests in general were found to be consistent with scuffing temperatures varying from 194°C to 216°C, giving an average of 202°C ± 7°C (±3%). The presence of oil on the specimens showed that scuffing in these tests was not simply due to the exhaustion of oil at the surface by evaporation, though the wear scar appeared to be free of oil. A temperature of 150°C was therefore chosen for the tests, as this is midway between the lowest friction coefficient at 100°C and the scuffing temperature at 200°C. In passing, we may note that the scuffing temperatures found here are about 50°C higher than those observed by Mills and Cameron [24] for stearic acid lubrication of steel/steel contacts.

The influence of temperature on the properties of the lubricant in terms of friction coefficient is shown in Fig. 5, and the variation of average friction coefficient with temperature was also found to be very consistent for the different tests, highlighting the repeatability of the test method.

4. Results

4.1. Influence of surface finish on friction

It is evident from Fig. 6 that there is an influence of surface finish on the average friction coefficient, with

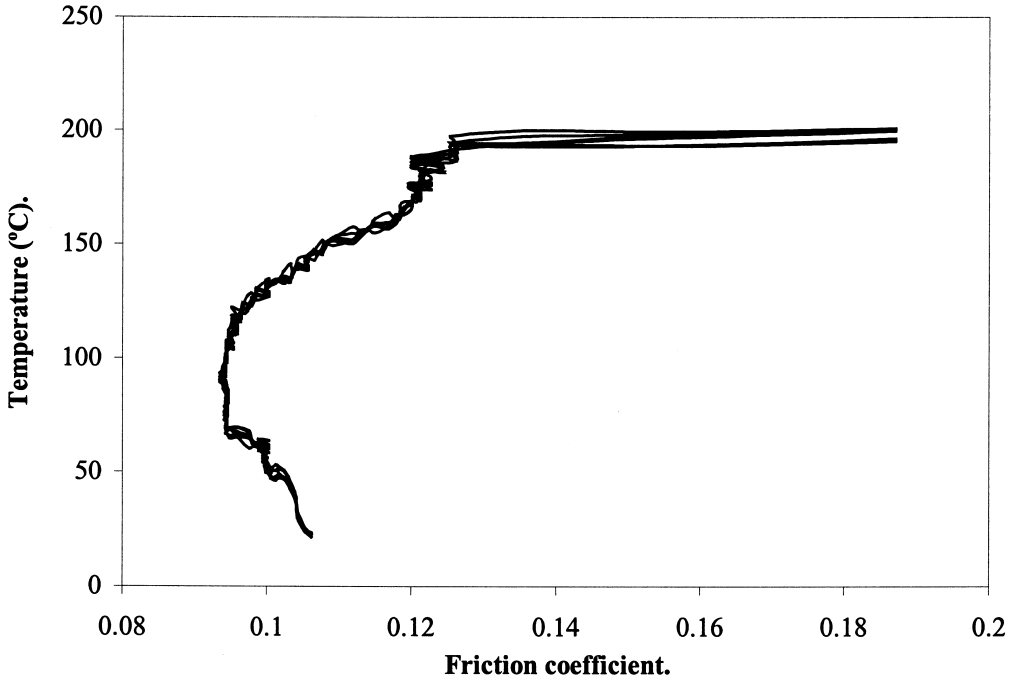

Fig. 5. Friction coefficient vs. temperature using 1% stearic acid.

smoother surfaces generally giving a lower friction coefficient. However, in the tests on the lightly polished bore specimens (5.20°) and the standard bore specimens (5.70°) the initial friction coefficient decreases over the first 100 s, whilst for the highly polished specimen (0.69°), it increases. These trends could be the result of a decrease in the rms asperity slope of the specimens as they run in [4]; but the increase in friction coefficient, in the case of the highly polished specimen, may also be due to the thick chemically absorbed ferric stearate film formed prior to testing during the heating period, being worn down within the first few strokes to a thinner film, as described by Bowden and Tabor [15].

During the scuffing tests, it was found that the finish on the piston ring changed little, but that the liners became smoother, with lower asperity slopes. There was no ob-

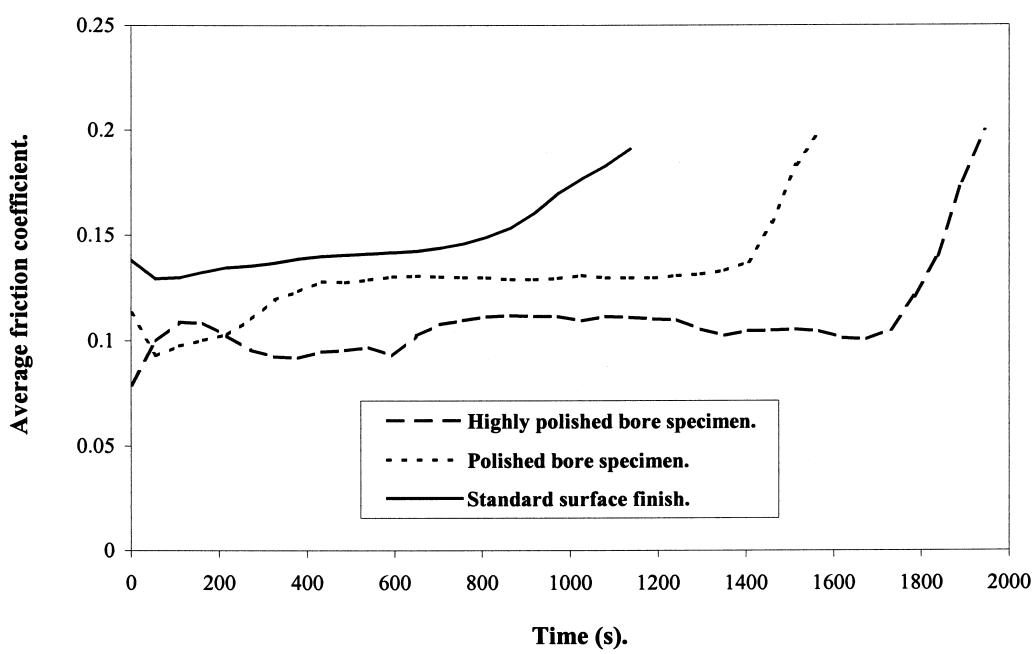

Fig. 6. Typical scuffing tests carried out on bore specimens with different surface finishes.

servable surface damage on either the ring or bore specimens normally associated with scuffing. In earlier tests where the scuffing limit was not well determined, severe wear was observed on both the ring and bore though no material transfer was observed. In these tests the friction coefficient rose and fell abruptly, resulting in a very jagged friction trace. At the end of every test, the combined rms asperity slope of ring and liner, determined as in Ref. [4], had fallen to the range 0.7°–1.7°, though initially it ranged from 1.7° to 6°. Fig. 7 shows these results (experimental points) plotted as friction coefficient against rms slope at 5% bearing area. The tests that scuffed are shown as circles. Six tests that did not scuff are also shown. The diamond data points are for a specimen so highly polished that it was covered with graphite, which prevented scuffing over a 3-h period. The other five tests (square data points) were stopped just before scuffing occurred. The triangle data points represent two tests carried out with standard bore specimens and highly polished ring specimens.

Theoretical friction curves are also plotted for a range of boundary film defects. The value of μ_0 is taken to be 0.003, which corresponds to the value measured for the stearates [15] which will form by reaction of the stearic acid lubricant with iron at the test temperature of 150°C, [13,14]. In previous work [4], the experimental results correlated well with $f = 0.08$, which is shown as a bold line. This also correlates reasonably well with the initial friction values measured here (solid data points), but does not predict the friction at the end of the tests (open data points).

The theory will, however, predict the friction at the end of the tests if it is supposed that f rises, perhaps due to exhaustion of the lubricant during the test; but to explain all the results observed, it must be supposed that f can rise to 0.5. It is difficult to accept such a high value of f, which hardly squares with the observation that the liner is undamaged after the test; so an alternative explanation should be sought.

4.2. Influence of surface finish on scuffing resistance

The scuffing resistance of a particular combination of ring, liner and lubricant can be measured in terms of time to scuff. This was found to be affected by surface finish. For standard and rough liners, the parameter, which correlated best with time to scuff, was rms asperity slope at 50% bearing area. This is shown in Fig. 8 (solid data points). However, when the liner was polished (open data points), the time to scuff no longer increased, but became very scattered, with, if anything, a tendency to decrease for smoother surfaces. Thus, there would seem to be two distinct trends: for specimens with an rms asperity slope greater or equal to 5°, scuffing resistance increases with decreasing rms asperity slope; but the scuffing time of specimens with an rms asperity slope less than or equal to 4° is very scattered. It may be that an intermediate range of

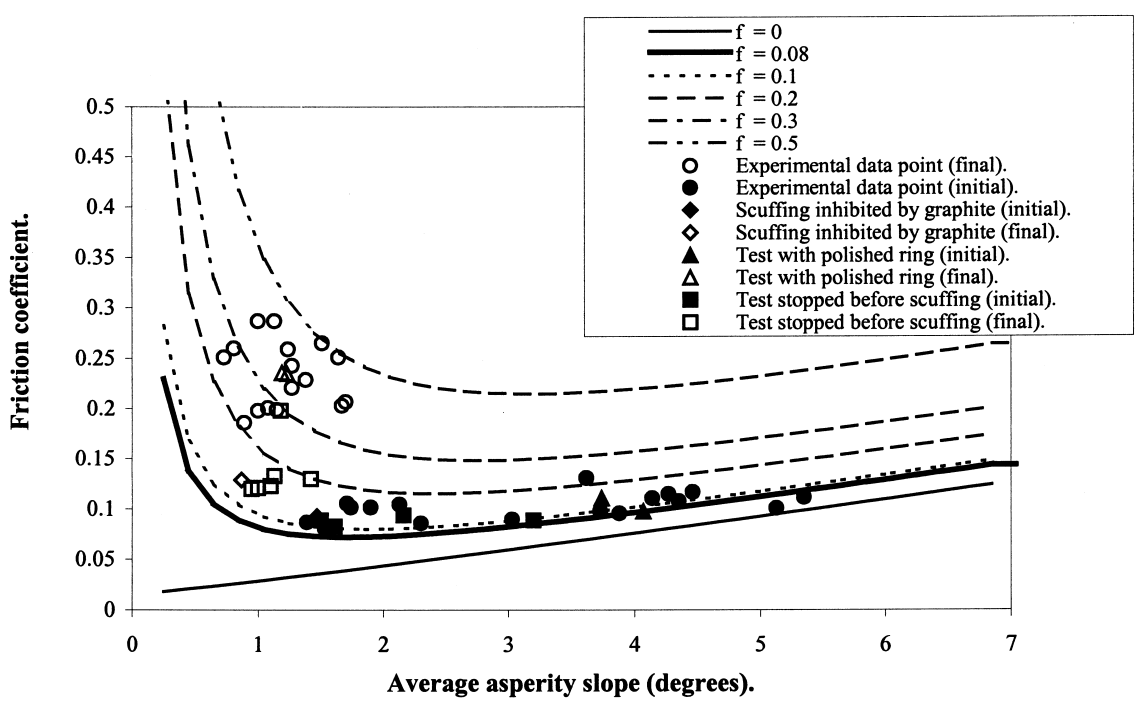

Fig. 7. Comparison of theoretical and experimental friction, where black data points represent the initial friction and the white data points the final friction measured.

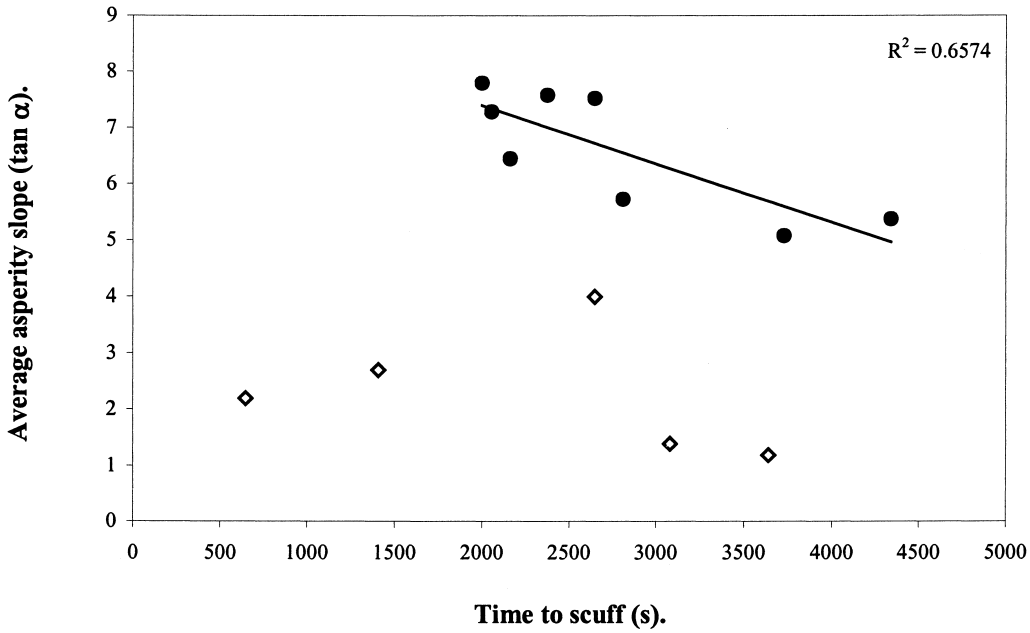

Fig. 8. Correlation of surface finish in terms of average asperity slope at 50% bearing area with scuffing time.

roughness results in the best scuffing resistance, as others have also suggested [2,3].

5. Discussion

A glance at Fig. 7 shows that the relationship predicted between asperity slope and friction coefficient is far from linear. One consequence of this is that where asperity slopes vary about a mean, the friction that would be predicted from the whole slope distribution may be different from that predicted using simply the rms slope. The extent of this effect was investigated in the following way. For a random selection of the profiles studied, the slope distribution, normalised by the rms slope, was measured as a 30 bar histogram. For each case a value of $f = 0.08$ was used as before, and the friction coefficient was calculated, weighted by the probability of finding the slope. The effect on friction coefficient of changing the value of the rms slope was then calculated for each of the slope distribu-

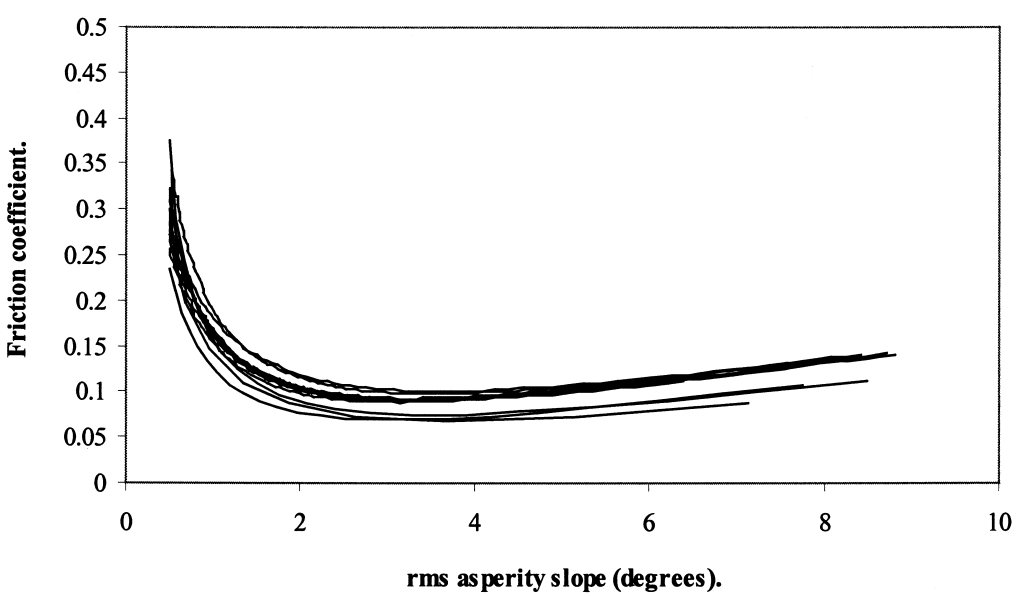

Fig. 9. Friction vs. rms slope using measured slope distributions, $f' = 0.08$.

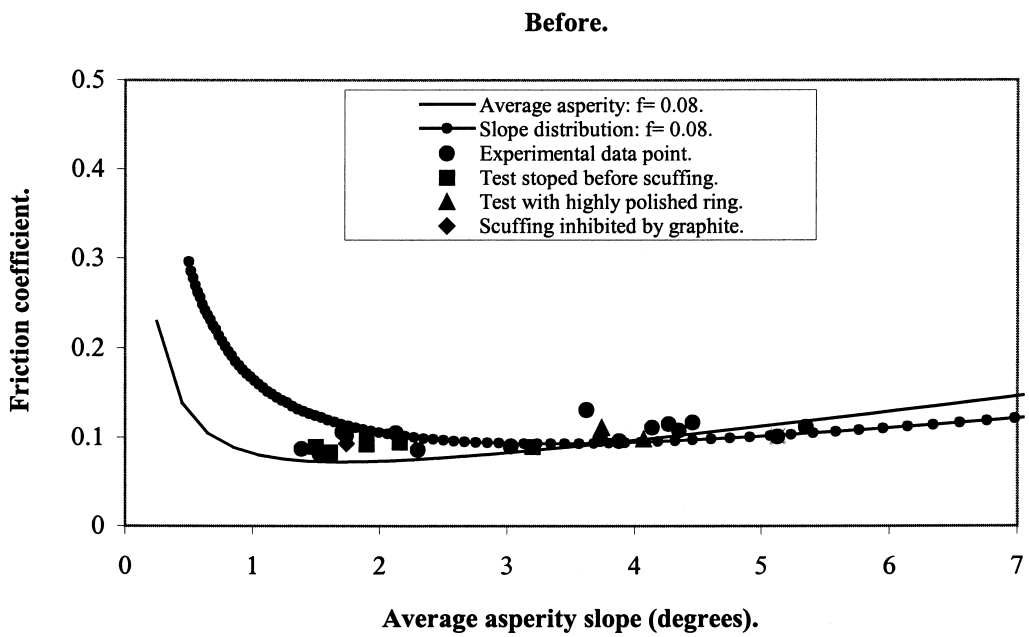

Fig. 10. Friction coefficient measured and predicted at the start of the test using slope distribution and average slope ($f = 0.08$).

tions. The result is shown in Fig. 9. Comparing these curves with the curve for $f = 0.08$ in Fig. 7 shows that at low slopes the friction is now sensibly higher than if the rms slope is used alone, whilst at slopes of over 5° the distribution predicts a lower friction.

Fig. 10 shows how the friction calculated using a typical slope distribution compares with the initial friction measurements and with the friction calculated using simply the rms slope. The value of f is 0.08 as before, and agreement is within experimental error, with most of the points lying on or between the two theoretical curves. However, the friction measured at the end of the tests still implies some kind of increase in f, though much more modest than before. Fig. 11 shows how the measured results compare with the friction calculated assuming distributed slopes and $f = 0.2$, and assuming $f = 0.08$ and the rms slope. Once again, nearly all the experimental results lie between the two curves, indicating that the observed rise in friction can be accounted for by a fairly modest increase in film defect.

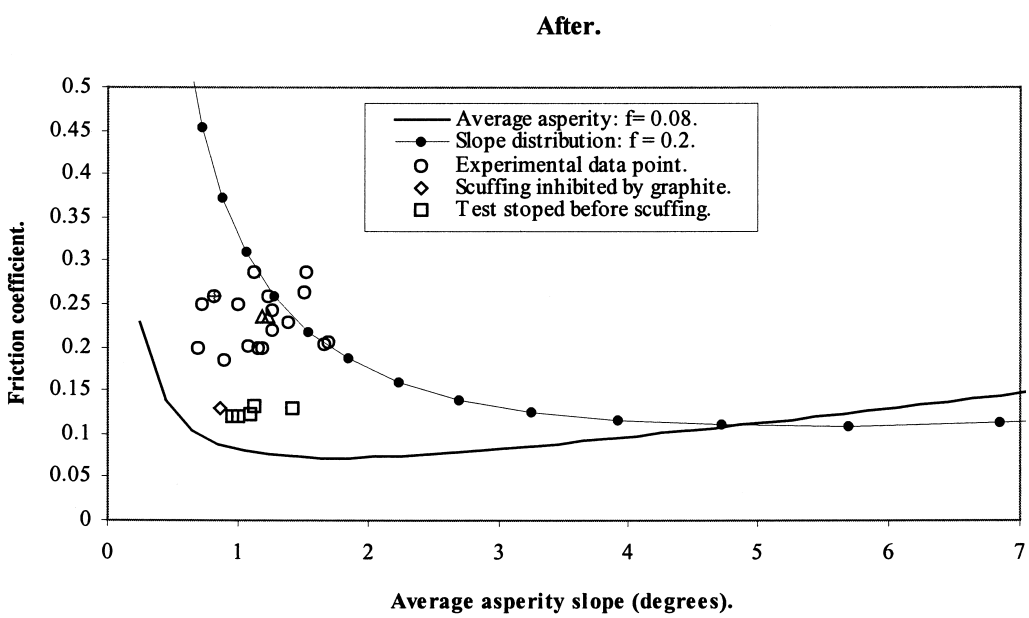

Fig. 11. Friction coefficient measured and predicted at the end of using slope distribution ($f = 0.20$) and average slope ($f = 0.08$).

The rise in friction observed at the end of the scuffing tests seems thus to be linked to two phenomena: a reduction in asperity slope, and in most cases, a modest reduction in the coverage of the rubbing surfaces by the boundary film. Judging by the fairly rapid rise in friction at the end of the tests, the two effects probably occur in sequence: first, the surfaces become polished and sensitised to film depletion; then, when the small amount of oil initially present begins to be exhausted, the friction rises quite rapidly and the test is stopped. The high friction phase of the test is then too short to cause any significant damage to the sliding surfaces, which emerge from the apparatus highly polished. If, at the end of a test, the surfaces of the specimens were cleaned in petroleum ether and relubricated, they would run again for approximately the same length of time before failing once more, indicating that exhaustion of the lubricant is an important effect. However, if they were simply cooled to room temperature and restarted, the coefficient of friction would fall to about 0.12 (25% higher than before failure). This indicates that boundary lubrication recovers at low temperature, but that the smoothing of the specimens has caused the coefficient of friction to rise.

Nothing has been said about the chemical characteristics of the boundary film. The model presented here postulates that it has certain mechanical characteristics, which would result from a mixture of organic and inorganic phases. The organic phase would have a shear strength following Eq. (4), giving an overall shear strength following Eq. (8) when combined with an inorganic phase. In the text we have treated this inorganic phase as though it were composed of the small metal/metal contacts postulated by Bowden and Tabor [14,15]. However, the same type of behaviour could be expected from the thicker films postulated by Mills and Cameron [24] if they consist of a mixture of oxide and organic matter. The fractional defect f, which we have postulated to have the value of 0.08, is a mathematical means of allowing for the mechanical effects of such an admixture of phases. Further investigation of the nature of these films would be useful to provide a better understanding of how their mechanical properties relate to their composition.

6. Conclusions

(1) A test has been developed to measure the sensitivity of different ring/liner combinations to scuffing.

(2) The friction measured in these tests can be related to the measured slope distributions of the asperities in contact and the properties of the boundary film with an elastoplastic asperity contact model.

(3) Scuffing finally occurs when a critical combination of polishing and film breakdown occurs, which can be predicted by the model.

7. Nomenclature

ABCDE	Points defining slip-line field (Fig. 5).
a	Contact length of front face of sliding wedge
E_1, E_2	Young's moduli of materials in contact
E^*	Reduced Young's modulus of contact
F_n	Normal force per unit width on wedge
F_t	Tangential force per unit width on wedge
f	Fractional defect of boundary film
H_v	Vickers hardness of softer solid
k_s	Shear yield strength of softer solid in contact
p_a	Mean pressure on front face of wedge
$p(x)$	Pressure on wedge a distance x from its apex
p_m	Maximum pressure on front face of wedge
x	Horizontal distance from the apex of the wedge
x_m	Value of x when $p(x) = p_m$
Y	Tensile yield strength of softer material
$\alpha, \varepsilon, \eta, A$	Angles defined in slip-line fields (Fig. 1)
θ	Friction angle on attack face of wedge ($\tan\theta = \tau/p$, cf. Fig. 6)
μ	Coefficient of friction
μ_0	Intrinsic coefficient of friction of boundary film
ν_1, ν_2	Poisson's ratios of materials in contact
σ_l	Rms slope of liner asperities
σ_r	Rms slope of ring asperities
τ	Shear strength of real contact area
τ_0	Residual shear strength of boundary film
τ_f	Shear strength of boundary film ($\tau_f = \mu_0 + \tau_0$)

Acknowledgements

The authors acknowledge with gratitude the financial sponsorship of the experimental part of this work by La Direction de l'Ingénierie des Matériaux of Renault.

References

[1] W. Hirst, J.V. Stafford, Transition temperatures in boundary lubrication, Proc. Inst. Mech. Eng. 186 (1972) 15–72.
[2] W. Hirst, A.E. Hollander, Surface finish and damage in sliding, Proc. R. Soc. London, Ser. A 337 (1974) 379–394.
[3] C.Y. Poon, R.S. Sayles, The classification of rough surface contacts in relation to tribology, J. Phys. D: Appl. Phys. 25 (1992) A249–256.
[4] A.A. Torrance, J. Galligan, G. Liraut, A model of a smooth hard surface sliding over a softer one, Wear 212 (1997) 213–220.
[5] C.R. Knight, H. Weiser, The lubrication requirements of European automotive diesel engines, S.A.E. paper 760721 (1976).
[6] J.A. McGeehan, A single-cylinder high BMEP engine for evaluating

lubricant effects on piston deposits, ring wear, oil consumption, and bore polishing, SAE paper 800437 (1980).
[7] J. Ayel, F. Roux, G. Tahon, Mécanisme de l'usure par polissage des cylinders de moteurs diesel, Rev. Inst. Fr. Pet. 37 (1982) 531–573.
[8] W.P. Dong, E.J. Davis, D.L. Butler, K.J. Stout, Topographic features of cylinder liners — an application of three dimensional characterisation techniques, Tribol. Int. 28 (1995) 453–463.
[9] J.V. Wilson, J.R.D. Callow, Cylinder bore polishing in automotive diesel engines — a progress report on a European study, SAE paper 760772 (1976).
[10] J.M. Challen, P.L.B. Oxley, An explanation of the different regimes of friction and wear using asperity deformation models, Wear 53 (1979) 229–243.
[11] K. Komvopoulos, N. Saka, N.P. Suh, Ploughing friction in dry and lubricated metal sliding, ASME J. Tribol. 108 (1986) 301–313.
[12] R.M. Mortier, S.T. Orszulik, The Chemistry and Technology of Lubricants, Blackie, London, 1997.
[13] Y. Wakuri, T. Hamatake, M. Soejima, T. Kitihara, Piston ring friction in internal combustion engines, Tribol. Int. 25 (5) (1992) .
[14] F.P. Bowden, D. Tabor, The Friction and Lubrication of Solids, Vol. 1, Oxford, 1950.
[15] F.P. Bowden, D. Tabor, The Friction and Lubrication of Solids, Vol. 2, Oxford, 1964.
[16] B.J. Briscoe, B. Scruton, F.R. Willis, The shear strength of thin lubricant films, Proc. R. Soc., Ser. A 333 (1973) 99–114.
[17] A.J. Black, E.M. Kopalinsky, P.L.B. Oxley, Sliding metal friction with boundary lubrication: an investigation of a simplified friction theory and of the nature of boundary lubrication, Wear 137 (1990) 161–174.
[18] A.A. Torrance, A. Parkinson, Towards a better surface finish for bearing materials, in: D. Dowson, M. Godet (Eds.), 19th Leeds–Lyon Symposium, Elsevier, 1993.
[19] K.L. Johnson, Contact Mechanics, Cambridge, 1985, pp. 113–115.
[20] Galligan, Friction of piston rings–cylinder bores, Thesis, University of Dublin, 1998.
[21] A.A. Torrance, A simple datum for measurement of the Abbott curve of a profile and its first derivative, Tribol. Int. 30 (1997) 239–244.
[22] M.J. Neale, Piston ring scuffing — a broad survey of problems and practice, Proc. Inst. Mech. Eng. 185 (1971) 21–32.
[23] W.J.S. Grew, A. Cameron, Thermodynamics of boundary lubrication and scuffing, Proc. R. Soc., Ser. A 327 (1972) 47–59.
[24] T.N. Mills, A. Cameron, Basic studies on boundary, EP and piston ring lubrication using a special apparatus, ASLE Trans. 25 (1982) 117–124.